Epilepsia, **48**(6):1179–1183, 2007
Blackwell Publishing, Inc.

Brain Mapping of Epileptic Activity in a Case of Idiopathic Occipital Lobe Epilepsy (Panayiotopoulos Syndrome)

*Alberto J.R. Leal, †Sofia Nunes, ‡António Martins §Mário Forjaz Secca, and ¶Constança Jordão

*Department of Neurophysiology, Hospital Júlio de Matos, Lisbon, Portugal †Departments of Pediatrics and ‡Neurology, Hospital Fernando Fonseca, Amadora, Portugal §Department of Physics, New University of Lisbon, Caparica, Portugal ¶Department of Neuroradiology, Hospital Egas Moniz, Lisbon, Portugal

Summary: The Panayiotopoulos type of occipital lobe epilepsy has generated great interest, but the particular brain areas involved in the peculiar seizure manifestations have not been established. We studied a patient with the syndrome, using high-resolution EEG and simultaneous EEG and functional magnetic resonance imaging (fMRI). Resolution of the scalp EEG was improved using a realistic spline Laplacian algorithm, and produced a complex distribution of current sinks and sources over the occipital lobe. The spike-related blood oxygen level dependent (BOLD) effect was multifocal, with clusters in lateral and inferior occipital lobe and lateral and anterior temporal lobe. We also performed regional dipole seeding in BOLD clusters to determine their relative contribution to generation of scalp spikes. The integrated model of the neurophysiologic and vascular data strongly suggests that the epileptic activity originates in the lateral occipital area, spreading to the occipital pole and lateral temporal lobe. **Key Words:** Epilepsy—Occipital lobe—BOLD—Childhood.

The most common syndrome of idiopathic occipital lobe epilepsy (IOLE) has been a source of puzzling questions since its description by Panayiotopoulos (Panayiotopoulos, 1989). The cardinal ictal manifestations of vomiting, eye deviation and long periods of interruption of consciousness, with rare visual symptoms, constitutes an unusual constellation of symptoms and up to now very little is known about the particular cortical structures involved in their generation. The consistent clinical picture in affected children suggests that a common epileptic network is at work and persists with little change throughout the evolution of the syndrome. The variability of the EEG (Panayiotopoulos, 2002) has resulted in a failure to provide consistent generators in this type of epilepsy. Attempts to improve its localizing capabilities, and also of MEG, using source analysis (Kanazawa et al, 2005; Yoshinaga et al, 2005; Yoshinaga et al, 2006) have resulted in localizations that do not explain the peculiar clinical symptoms and the lack of visual manifestations. In this study we perform a detailed brain mapping of a single case and demonstrate how this data provide a better integration of clinical and EEG data.

Accepted February 11, 2007.
Address correspondence and reprint requests to Alberto J.R. Leal at Department of Neurophysiology, Hospital Júlio de Matos, Av[a] do Brasil nr 53, 1749-002 Lisbon, Portugal. E-mail: ajrleal@hjmatos.min-saude.pt
doi: 10.1111/j.1528-1167.2007.01119.x

CASE REPORT

A healthy 11-year-old boy, with no previous history of seizures, was found with the eyes turned to one side, not responding to verbal stimulation and a pale face, while resting in the beach. He recovered normal behavior after a few minutes. Hours later, while resting in a sofa, he repeated the symptoms, which also lasted for a few minutes. Medical evaluation at an emergency department half an hour later failed to find any abnormality and he was discharged with an EEG booked for the next day.

The EEG revealed almost continuous spike activity over the left posterior areas, and he was admitted to the Intensive Care Unit for vigilance, despite the fact that he remained alert and with a normal neurological status. No evidence supporting persisting clinical seizures was found.

An ambulatory device using the full 10–20 system was used to monitor continuously the EEG (24 h). The prominent left posterior spike activity with the eyes closed was confirmed, as well as its striking decrease while recording with the eyes open, which led to he diagnosis of IOLE. The patient was medicated with sodium valproate and remains seizure-free after 6 months.

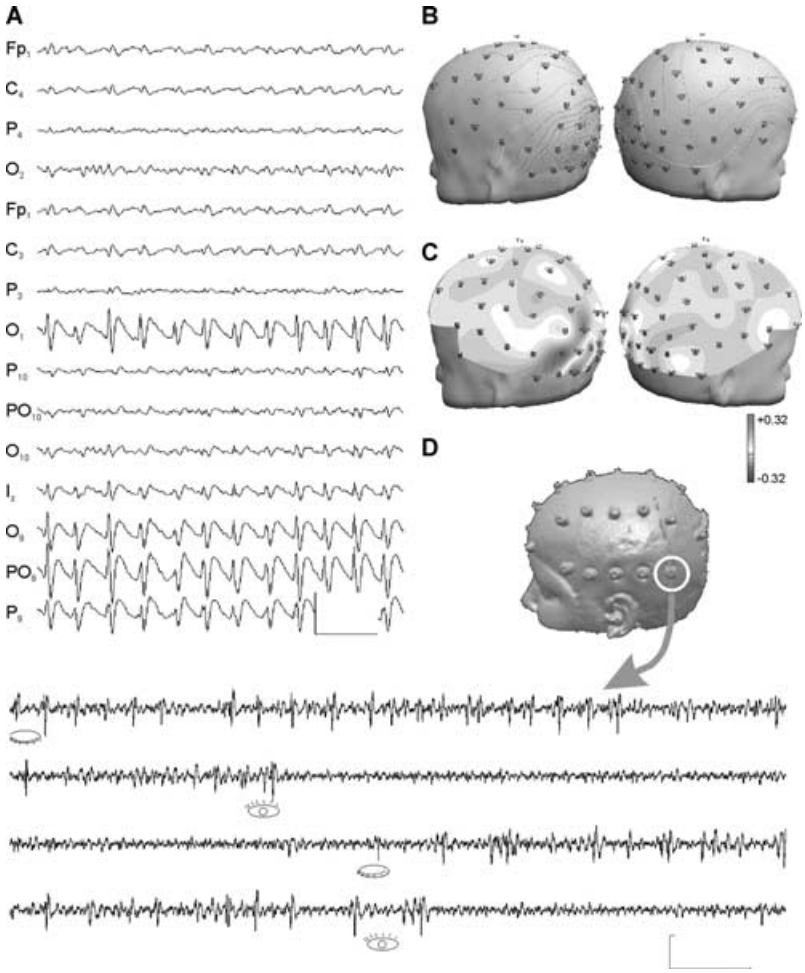

FIG. 1. (A) Subsample of the 64-channel EEG recording, demonstrating almost continuous spike activity over the posterior derivations on the left hemisphere with the eyes closed. Vertical bar is 200 μV, horizontal bar 1 s. **(B)** Dipolar distribution of the scalp potential obtained with 64 channels over a realistic head surface and with average reference. **(C)** Map of the spline Laplacian, showing current sources and sinks with a complex spatial distribution over the posterior left hemisphere. Color scale bar in μV/sqm. **(D)** EEG obtained inside the scanner, demonstrating a strong modulation of the spike activity with opening and closing of the eyes (electrode T5). Vertical bar 256 μV, horizontal bar 3.1 s.

METHODS

To improve the spatial mapping of the epileptic activity on the scalp a high-resolution (64 electrodes), 2-h long recording, was done using a special AgCl electrode cap (Fig. 1B), a 256-Hz sampling rate and filters between 0.5 Hz and –70 Hz. The electrode positions in the scalp were determined using an electromagnetic digitizer (Polhemus, Colchester). A realistic spline Laplacian montage as implemented in the ASA 2.2 software package (ANT, Enschede) was applied.

The patient was later submitted to a 1-h session of simultaneous EEG/fMRI recording, using a special EEG cap (Fig. 1D) designed for passive recording inside the scanner (Maglink system from Neuroscan, El Paso, TX, U.S.A.). A 37 channels EEG DC recording with a sampling rate of 1000 Hz and low pass filter at 70 Hz was used. The echo planar imaging (EPI) artifacts were removed with the Scan 4.3.3 software package (Neuroscan), allowing a clear detection of spike onset (Fig 1D). Four blocks of 100 brain volumes, each one made of 16 EPI images (in plane resolution 3.75 mm and slice thickness of 7 mm, no spacing; echo time 50 ms; flip angle of 90°), were obtained with a TR = 3 s, corresponding to periods of 5 min of simultaneous EEG/fMRI. A head 3D T1 spoiled gradient recalled gradient (SPGR) sequence was also acquired (in plane resolution of 0.94 mm and slice thickness of 1.3 mm for a field of view of 24 × 24 cm). Images were obtained in a 1.5T GE CVi/NVi scanner.

EPI sequences were corrected for slice acquisition time and movement, and smoothed with a Gaussian kernel of full width at half-maximum of 5 mm, using the FEAT 5.63 software package (Smith et al., 2005). The initial two sequences were obtained while the patient remained with the eyes closed, but in the last two the patient alternated periods of 30 s with eyes open and closed (Fig. 2A). EPI volumes were then submitted to independent component analysis (ICA) using the infomax algorithm (Bell and Sejnowski, 1995) as implemented in the GIFT 1.3b package (available at http://icatb.sourceforge.net/). The independent components (IC) were then submitted to a temporal sorting by the multiple regression coefficients obtained by adjusting their time courses to a regressor constructed by the time of occurrence of the spikes convolved with a standard gamma hemodynamic response function (Fig. 2A) obtained from visual evoked potentials (Huettel

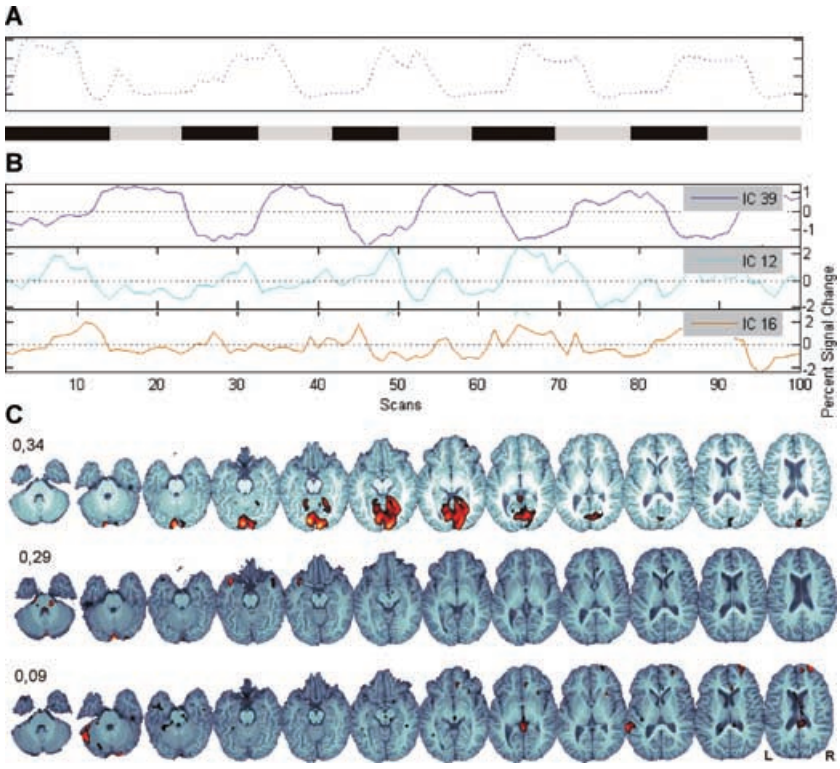

FIG. 2. (A) Temporal evolution of the opening and closing of the eyes (below: black–closed, gray–open) and the associated amount of spike activity (convoluted with a standard gamma function), above. **(B)** Time course of the three independent components more clearly correlated with the opening/closing of the eyes and with the occurrence of spikes. Component 39 is produced by visual cortex activation, while components 12 and 16 are spike-related. **(C)** Spatial ICs, sorted by the coefficients of the multiple regression (number on the left) fitting the components to the number of spikes regressor in **(A)**, above. The images were thresholded with a $z = 2.3$.

et al., 2004). The components with the highest covariance with the previous regressor were selected for further analysis (Fig. 2B), and images were thresholded with a z-score of 2.3. The blood oxygen level dependent (BOLD) images were registered to the 3D T1 sequence using FLIRT 5.0 (Jenkinson et al, 2002).

Determination of the relative contribution of the BOLD activation areas was done by seeding regional dipoles in the center of the BOLD clusters and determining the temporal contribution of each source to the average spike in the scalp, using a three-shell spherical volume conductor model.

RESULTS

The long-term EEG demonstrated a single and stable topography of the spike activity over the left occipital lobe, a feature confirmed with the high-density recording (Fig. 1A,B). This topography at spike peak was dipolar (Fig. 1B) but the use of a realistic spline Laplacian reference improved the spatial resolution and demonstrated a more complex configuration of sources and sinks of current over the left occipital lobe, suggesting that multiple cortical generators are involved in spike production. Also, because of the well-known selectivity of the Laplacian to superficial sources (Nunez et al., 1994), this result supports involvement of the more superficial occipital cortex in epileptic activity.

The spikes recorded inside the scanner demonstrated a strong modulation with opening and closing of the eyes (Fig 1D), allowing creation of a baseline (eyes open) condition and an activated state (eyes closed). The absence of baseline in the two sequences acquired with the eyes continuously closed prevented detection of significant BOLD effect.

The ICA procedure used did not require any information on the time of occurrence of the spikes or the opening and closing of the eyes, but recovered three components (of more than 50) whose activation exhibited a strong temporal correlation with those two regressors of interest (Fig. 2A,B). The component more clearly time-locked to the opening and closing of the eyes corresponded to activation of the primary visual areas (Fig. 2C) and reflects the normal activation of the visual pathway. The other two components showed consistent activation with the eyes closed and are time-locked to the occurrence of spikes, expressing the BOLD activation due to these pathological events (Fig. 2C). The remaining components either expressed known artifacts or did not show a compatible modulation of the temporal activation.

One of the selected components expressed a maximum at the left occipital pole and two secondary ones at both temporal poles (Fig. 2C, middle). The other produced BOLD activation of the left temporal–occipital junction, the lateral left temporal lobe and also in the right frontal lobe (Fig. 2C, below). Overall a widespread, spike induced, BOLD activation of the left occipital and temporal lobes is suggested, supporting either a diffuse epileptogenic area or significant spread of the interictal activity.

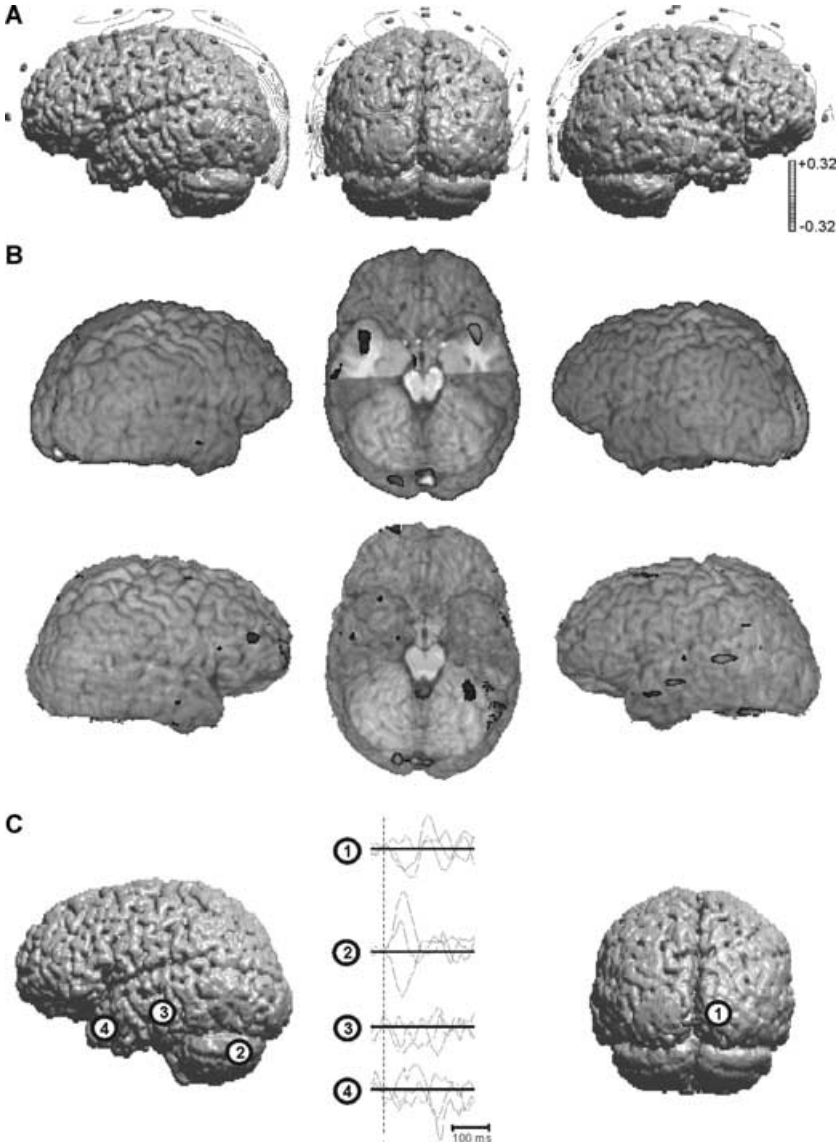

FIG. 3. (A) Spline Laplacian map at the peak of an average spike, represented over a 3D rendering of the patient brain. The complex distribution suggests a multifocal and extended epileptogenic area over the left occipital lobe. Red represents current sources, while blue represents current sinks (color scale bar in μV/sqm). **(B)** 3D representation of the BOLD activation clusters co-registered with the patient brain for the two ICs spike related. The more posterior cluster of IC12 (above) and the occipital–temporal junction cluster of IC16 (bellow) are compatible with sources suggested by the Laplacian map in **(A)**, but no electrical activity is apparent near the remaining BOLD cortical clusters. **(C)** Regional dipole seeding at the BOLD clusters allows an estimate of the temporal contribution of each activation area to the scalp average spike. The recovered activation curves (middle) suggest an origin of epileptic activity in the occipital–temporal junction (2) source and rapid spread to the nearby occipital pole (1) and temporal lobe (3 and 4).

There is spatial overlap of BOLD cortical activation with the Laplacian mapping for the posterior occipital regions (Fig. 3A,B), but at frontal and more anterior temporal areas no scalp electrical activity can be demonstrated in the Laplacian montage (Fig. 1C and 3A). The average reference montage does not show significant electric activity at these areas either (Fig. 1B).

The analysis of the seeded dipole activation curves suggests that the lateral and inferior occipital area originate the epileptic activity, which later spreads to the occipital pole and temporal lobe (Fig. 3C).

DISCUSSIONS

The normal neurological status as well as the lack of any abnormality in the brain MRI supports the diagnosis of idiopathic epilepsy, which is also supported by the EEG demonstration of abundant and high amplitude posterior spike activity.

The ictal manifestations of tonic deviation of the eyes, decreased consciousness and pallor are common features in the Panayiotopoulos type of IOLE, which associates autonomic manifestations with eye movement and consciousness disturbances (Ferrie et al., 2006). The absence of prominent autonomic manifestations, such as vomiting, is atypical but does not exclude the syndromic diagnosis (Ferrie et al., 2006). The alternative diagnosis of Gastaut type of IOLE seems unlikely because the usual ictal visual manifestations and preservation of consciousness in this syndrome are absent in our patient.

Most studies using source analysis to localize spike generators in this syndrome, either using EEG (Yoshinaga et al., 2006) or MEG (Kanazawa et al., 2005), have used such a dipolar distribution of the scalp potential to postulate a single dipole generator that they located near the

calcarine sulcus and the parietal–occipital sulcus. These results suggesting an epileptogenic area near the visual cortex are not compatible with the rarity of visual symptoms and are also not compatible with our results, which show a complex distribution of sources and sinks of current over the left occipital lobe. The spatial filtering properties of the Laplacian, which strongly favor superficial cortical sources (Nunez et al., 1994), further suggest that in our patient the epileptogenic area is extended and not focal, involving the pole and superficial lateral occipital cortex.

The lack of data on the characteristics of the BOLD response (Duann et al., 2002) in normal and epileptic tissue, which makes it difficult to choose the right parameters for a conventional model-based processing of the fMRI data, motivated us to use a data-driven approach that in previous studies produced results similar to the ones of the model-driven method (Nybakken et al., 2002; Quigley et al., 2002), but does not require apriori knowledge of model parameters. This approach seems particularly useful in the detection of the BOLD effect of interictal spikes, as those events are sometimes difficult to detect, resulting in decreased sensitivity of model-driven methods (Liston et al., 2006).

The occipital BOLD clusters show a good agreement with the Laplacian map, which suggests at least two cortical generators, one in the left pole and another one in the more lateral and inferior area (Fig. 3A,B). The BOLD activations over the temporal and frontal areas are not associated with a detectable scalp electrical activity.

The activation curves obtained by the dipole seeding at the BOLD activation clusters suggest that the scalp spikes originate in the lateral occipital lobe and spread to the pole and lateral temporal cortex of the same hemisphere. No contribution from other sources was apparent.

The previous results provide a tentative explanation of the peculiar ictal clinical manifestations of our patient. The interruption of consciousness can be attributed to epileptic propagation to the temporal lobe, while the eye deviation is likely to be due to the localization of epileptic activity to the occipital–temporal junction, a cortical area well known to be activated in smooth pursuit and saccadic eye movements (Petit and Haxby, 1999). The limited autonomic manifestations in our patient (pallor) offer little opportunity to determine the possible generators of more typical manifestations such as vomiting. Comparison of brain mapping in patients with diverse clinical manifestations within the same syndrome might offer an opportunity to determine the brain areas associated with particular symptoms.

Acknowledgments: The authors are grateful to Cristina Menezes, Daniel Carvalho, Rita Pinto, and Elisabete Lage for technical support and to Prof. Alexandre Andrade and Rosalina Fonseca for revision of the paper.

REFERENCES

Bell AJ, Sejnowski TJ. (1995) An information-maximization approach to blind separation and blind deconvolution. *Neural Computation* 7: 1129–1159.

Duann JR, Jung TP, Kuo WJ, Yeh TC, Makeig S, Hsieh JC, Sejnowski TJ. (2002) Single-trial variability in event-related BOLD signals. *Neuroimage* 15: 823–835.

Ferrie C, Caraballo R, Covanis A, Demirbilek V, Dervent A, Kivity S, Koutroumanidis M, Martinovic Z, Oguni H, Verroti A, Vigevano F, Watanabe K, Yalcin D, Yoshinaga H. (2006) Panayiotopoulos syndrome: a consensus view. *Developmental Medicine and Child Neurology* 48: 236–240.

Huettel S, McKeown J, Song A, Hart S, Spencer D, Allison T, McCarthy G. (2004) Linking hemodynamic and electrophysiological measures of brain activity: evidence from functional MRI and intracranial field potentials. *Cerebral Cortex* 4:165–173.

Jenkinson M, Bannister PR, Brady JM, Smith SM. (2002) Improved optimization for the robust and accurate linear registration and motion correction of brain images. *Neurimage* 17:825–841.

Kanazawa O, Tohyama J, Akasaka N, Kamimura T. (2006) A magnetoencephalographic study of patients with Panayiotopoulos syndrome. *Epilepsia* 46: 1106–1113.

Liston AD, De Munck JC, Hamandi K, Laufs H, Ossenblok P, Duncan JS, Lemieux L. (2006) Analysis of EEG-fMRI data in focal epilepsy based on automated spike classification and signal space projection. *Neuroimage* 31: 1015–1024.

Nunez PL, Silberstein RB, Cadiush PJ, Wijesinghe J, Westdorp AF, Srinivasan R. (1994) A theoretical and experimental study of high resolution EEG based on surface Laplacians and cortical imaging. *Electroencephalography and Clinical Neurophysiology* 90:40–57.

Nybakken GE, Quigley MA, Moritz CH, Cordes D, Haughton VM, Meyerand ME(2002) Test-retest precision of functional magnetic resonance imaging processed with independent component analysis. *Neuroradiology* 44: 403–406.

Panayiotopoulos CP. (1989) Benign childhood epilepsy with occipital paroxysms: a 15-year prospective study. *Annals of Neurology* 26: 51–56.

Panayiotopoulos CP. (2002) *Panayiotopoulos syndrome: a common and benign childhood epileptic syndrome*. John Libbey, London.

Petit L, Haxby JV (1999) Functional anatomy of pursuit eye movements in humans as revealed by fMRI. *Journal of Neurophysiology* 82: 463–471.

Quigley MA, Haughton VM, Carew J, Cordes D, Moritz CH, Meyerand ME. (2002) Comparison of independent component analysis and conventional hypothesis-driven analysis for clinical functional MR image processing. *AJNR American Journal of Neuroradiology* 23: 49–58.

Smith SM, Beckmann CF, Ramnani N, Woolrich MW, Bannister PR, Jenkinson M, Matthews PM, McGonigle DJ. (2005) Variability in FMRI: a re-examination of intersession differences. *Human Brain Mapping* 24:248–257.

Yoshinaga H, Koutroumanidis M, Shirasawa A, Kikumoto K, Ohtsuja Y, Oka E. (2005) Dipole analysis in Panayiotopoulos syndrome. *Brain Development* 27: 46–52.

Yoshinaga H, Koutroumanidis M, Kobayashi K, Shirasawa A, Kikumoto K, Inoue T, Oka M, Ohtsuka Y. (2006) EEG dipole characteristics in Panayotopoulos syndrome. *Epilepsia* 47: 781–787.